Volume 69, Issue 2, 2025
Journal of Scientific Research
of
The Banaras Hindu University

Petrography and Laser Raman Characterization of Banded Hematite Jasper from Agori Formation of Mahakoshal Greenstone Belt

Akash Kumar Singh and Dinesh Pandit*

Department of Geology, Institute of Science, Banaras Hindu University, Varanasi - 221005, India, *Email ID: dpandit@hotmail.com

Abstract: **The Laser Raman Micro Spectroscopy (LRMS) technique has been used to analyzed ore forming processes in the Banded Iron Jasper (BHJ). Petrographic studies of BHJ sample indicates that variable amounts of cryptocrystalline silica rich matrix occur as jasper or chert associated with hematite crystals. Jasper and hematite phases display characteristics Raman Shift approximately 466 cm^{-1} and 1318 cm^{-1} attributed to vibrational stretching mode (Si-O-Si) and two-phonon longitudinal optical (2LO) vibrational modes (Fe-O). Here, we investigated the effects of the Raman mapping of hematite crystal in the silica rich matrix as jasper. Our results clearly demonstrate that crystallization of hematite crystals with jasper in the Agori Formation precursors sequentially required supersaturated Fe-rich and Si-rich solution, uniform temperature and pressure conditions in the Paleoproterozoic Ocean and atmosphere.**

Index Terms: **Raman, Japser, Hematite, Agori, Mahakoshal**

I. Introduction

The Laser Raman Micro Spectroscopy (LRMS) is a principal technique for characterizing minerals, providing insights into their molecular structure and chemical compositions (Mernagh & Trudu, 1993). This technique uses a laser beam to excite the sample, causing it to scatter light in a system that reveals evidence about its molecular vibrational modes. Raman spectroscopy is a molecular vibrational technique that relies on the inelastic scattering of photons (light) by the sample. When a laser beam interacts with the sample, some of the photons are scattered, and the scattered light is analyzed to determine the vibrational modes of the molecular structure or crystal lattice. Analyzing the scattered light to recognize atomic bonding and their molecular structure. This technique provides a non-destructive method for mineral identification at microscale to nanoscale domain, and is suitable in geological and scientific applications (Pasteris, 1997). Raman spectroscopy can be used to identify different varieties of iron ores and gangue minerals present in Banded Iron Formation (BIF). Characteristics Raman bands can be used to distinguish between various mineral phases. By investigating the Raman spectra, researchers can identify different iron oxides (like hematite, magnetite, goethite and maghemite) and other minerals (quartz, jasper, chalcedony, moganite, chert, tridymite, and cristobalite) present in the BIF.

The objective of this study is to understand, using LRMS with 532-nm wavelength excitation, the precipitation of euhedral hematite crystal in jasper as silica rich matrix in the BHJ sample of the Agori Formation in the Mahakoshal Greenstone Belt (MGB). The investigation focuses on the ore formation processes in the MGB, the specific mechanism of hematite crystal nucleation and crystal growth in the jasper.

II. Regional Geology

The Paleoproterozoic Mahakoshal Greenstone Belt (MGB) is one of the significant supracrustal or mobile belt of the Central Indian Tectonic Zone (CITZ). The MGB is ENE-WSW trending and constitutes a significant litho-tectonic unit in the Son-Narmada-Tapti (SONATA) Lineament (Shanker, 1991). The MGB is bounded by the Son-Narmada North Fault (SNNF) in the north and the Son-Narmada South Fault (SNSF) in the south. The lithostratigraphic sequence of the MGB is known as Mahakoshal Group (Fig. 1). The Mahakoshal Group constitutes the northern most components of CITZ limited by regional scale deep seated SNNF and SNSF also separated it from Vindhyan Basin and Proterozoic granitoids of CITZ in the north and south respectively. The MGB has a length of 600 km that stretches from Hoshangabad of Madhya Pradesh in the west to Palamau of Jharkhand in the east. It is made up of metasedimentary and

metavolcanic rocks classified into three major units such as Agori (=Saleemanabad), Parsoi and Dudhamaniya Formations in the ascending order (Misra et al., 2022). The lowermost units of the Mahakoshal Group, the Agori Formation comprises clastic and non-clastic sediments with occurrences of minor volcanics. Volcanic rocks in the MGB comprises tuffs with metabasic lenses, lenticular bodies of dolomite and impure marbles, and Banded Iron Formation (BIF). The BIF includes Banded Hematite Quartzite (BHQ), Banded Magnetite Quartzite (BMQ), Banded Hematite Jasper (BHJ) and quartzites. The BHQ or BMQ or BHJ trends ENE-WSW. The Parsoi Formation has thick succession of phyllite, schists, argillites, turbidites and metasedimentary sequences closed by the phase of intrusion of granites, syenites and series of mafic dykes. The Dudhamaniya Formation confined within the southern part of the MGB having metavolcanics of basic and ultrabasic lava (peridotitic lava and pillow basalts), epidiorite, agglomeration, phyllite and calc-chloritic schist and minor andesitic lava at top of lava pile, with associated dykes and ultrabasic plugs. Field observations shows that BIF layers have alternative bands of jasper, hematite, quartzites, chert and quartz stingers (Fig. 2a). The BIF also displays at least two stages of deformation, the first stage connected with breccia texture (Fig. 2b) and second stage of deformation is represented by different sets (intraclast and extraclast) of fracturing in rocks (Fig. 2c).

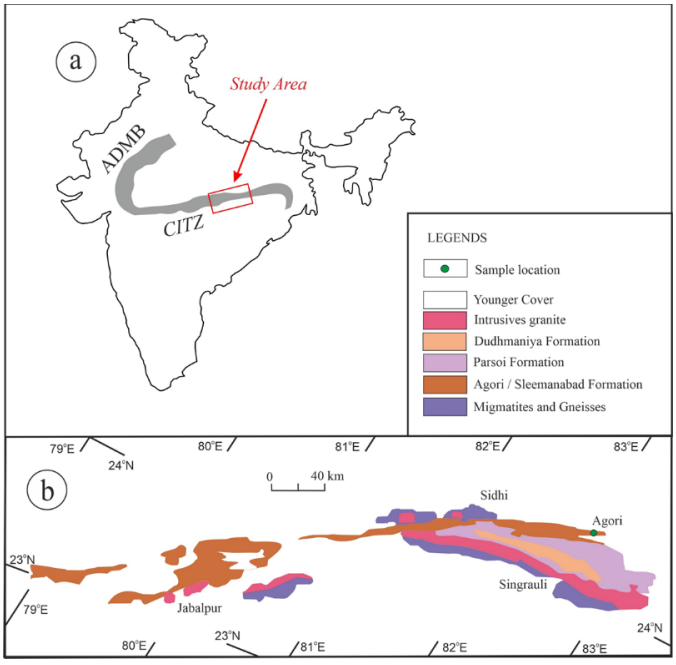

Fig. 1. (a) Map of India displays study area along the CITZ. (b) Geological map of Mahakoshal Greenstone Belt (modified after Roy et al., 2002) and also shown the sample location of the present study.

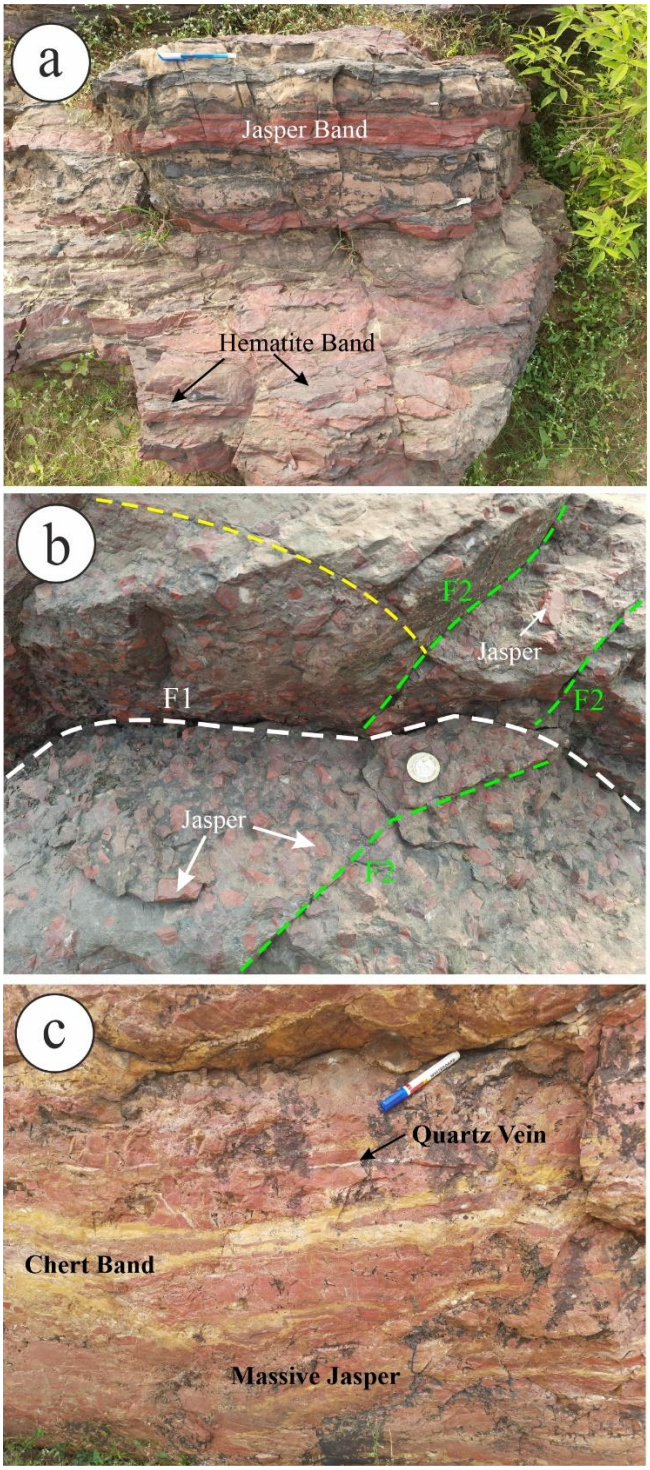

Fig. 2. Field photographs show exposed outcrops of Agori Formation in the Mahakoshal Group: (a) BIF layers have alternative bands of jasper very thick to thin banding (redish colour) and hematite very thin layers (colour steel gray to black, lusture metallic to submetallic), (b) deformed rock with breccia texture and numbers of intraclast fractures planes (F1) and extraclast fracture planes (F2) and (c) massive jasper with very fine streaks of quartz vein (white colour) and chert (pale yellow colour).

III. PETROGRAPHY

The Agori Formation of the MGB is hosting economically important iron ore deposits in the Central India. There are several occurrences of commercial grade iron ores in the BIF lithounits located in the state of Madhya Pradesh and Uttar Pradesh. These BIF units are layered sedimentary rocks rich in iron, primarily composed of alternating bands of iron-rich and iron-poor minerals. Petrographically, BIFs are characterized by the occurrence of iron oxides like hematite and magnetite, along with silica-rich bands (chert or jasper) and numerous extra minerals like clay minerals, and ankerite. Characteristic banding texture of iron ores in BIF on macroscales, mesoscales and microscales separated by silica-rich layers of chert or jasper. Macroscale bands of BIF packages are observed in centimeter (cm) to meter (m) scale thickness ranges between 50 to 100 µm (Fig. 2). In microscale, BIF displays alternating thick layers in centimeter (cm) called as mesobands and millimeter (mm) to micrometer (µm) thin layer known as microbands of predominantly chert and iron oxides (Egglseder et al., 2019). Important characteristic features of the BIF in the Agori Formation are the preservation of layering at all scales and are frequently accompanied by stratigraphic successions of phyllites and quartzites.

In this investigation, we emphasis on the process of formations of iron ores, which are naturally hard, massive and crumbly reddish-brown ores including of hematite bands associated with chert or jasper interlayers. Concurrent manifestations of hematite and jasper bands in the form of alternating layers signifies the characteristic features of Banded Hematite Jasper (BHJ). Randomly oriented micro-platy, subhedral to anhedral hematite crystals are fills the opening left overdue by withdrawal of gangue minerals such as quartz, jasper or chert. This iron ore type is commonly occurred as minor folding, small scale dislocations or local brecciation. The samples of BHJ show a varied range of grain shapes, sizes and intergrowths of alternative hematite bands and jasper bands. In thin sections, BHJ displays microbands, leading to strong crystal structure and microtextural changes.

Petrographic study under polarized reflected light mode displays alternate bands of white color hematite crystals and grey color of silicate-rich jasperous matrix (Fig. 3a). Black color hematite crystals with reddish-brown color silicate-rich matrix represented as jasper under plane polarized reflected light mode (Fig. 3b). The colouration in jasper is possibly due to very fine inclusions as cryptocrystalline grains of hematite above a threshold value of concentration. White color hematite crystals, light grey color massive hematite grains and pale green-brown color goethite occurs into silicate-rich dark grey to reddish-brown color jasperous matrix under polarized reflected mode (Fig. 3c).

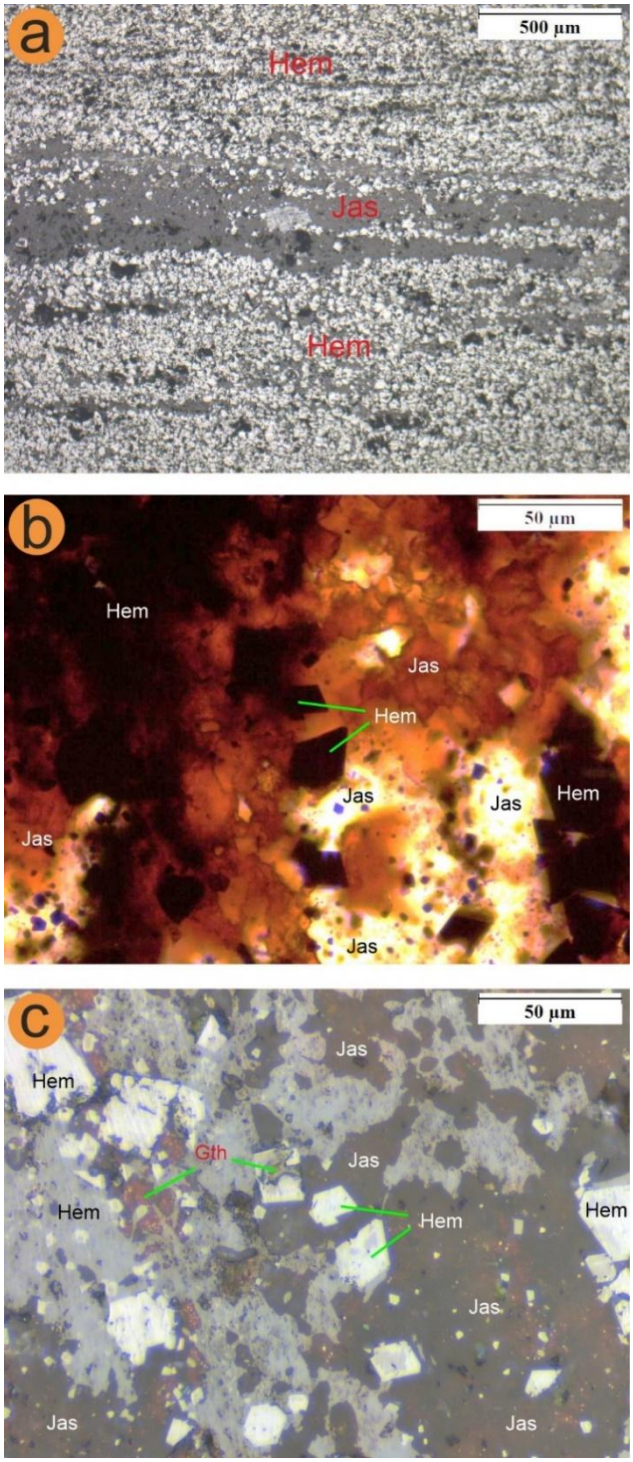

Fig. 3. Photomicrographs of BHJ from Agori Formation shows: (a) alternate bands of white color hematite crystals and dark grey color silicate-rich matrix as jasper under plane polarized reflected light mode, (b) black color hematite crystals and brownish color silicate-rich matrix as jasper shown under plane polarizing transmitted light mode and (c) white color hematite crystals and pale green color goethite present in silicate-rich dark grey to reddish-brown color jasperous matrix under polarized reflected light mode. Abbreviations: Hem – hematite, Jas – Jasper and Gth – goethite.

IV. THEORY AND METHODOLOGY

Polished thin sections of BHJ samples mounted on glass slides were studied using a polarizing microscope under transmitted and reflected light mode. Microtextural and microstructural characteristics of BHJ resembles the existence of hematite crystal and jasper as matrix associated with silicate rich matrix. However, minute inclusions (<10 μm) are very challenging to distinguish using a polarizing microscope. The widespread scope and enormous petrological, theoretical and methodological background on the characterization of iron ores associated with BHJ make it possible from a holistic approach.

Polished thin sections of BHJ samples mounted on glass slides were observed at Raman-SNOM-AFM Microscope System, Central Discovery Centre (CDC), Banaras Hindu University, Varanasi, India. Raman spectra were acquired using Confocal Raman imaging in combination with Scanning Near-field Optical Microscopy (SNOM) Make WITec, GmbH, Model: alpha 300-RAS. The combined Raman-SNOM microscope is also very beneficial for high-resolution Raman mapping, scanning and imaging techniques. The Raman-SNOM system was operated at 1 mW output power supply with a source of solid-state Neodymium-doped Yttrium Aluminum Garnet (Nd:YAG) laser emits green light at a wavelength of 532 nm (Pandit, 2024). The Raman spectral resolution regulates the capability to discriminate between closely spaced peak positions with an accuracy of 2 to 3 cm^{-1} relative to the internal standard at room temperature (Ferraro et al., 2003). Higher spectral resolution can improve the accuracy whereas it may decrease signal to noise ratio. In this study, Raman Shift analyzes broader spectral peaks, the accuracy might be lower, actually ±5 cm^{-1} or even higher.

RRUFF database offers a standard Raman scattering spectral library for the identification of oxides and silicate minerals (Lafuente et al., 2015). In this study, Raman spectra from the RRUFF database are used to identify the characteristics of Raman Shift (cm^{-1}) of common oxide minerals such as quartz, hematite, and jasper (Fig. 4). Raman spectra from the RRUFF database have been applied for qualitative databases used to recognize the diagnostic Raman Shift of common oxide minerals such as quartz and hematite. These Raman Shift of quartz (Liu et al., 1997) and hematite (Marshall et al., 2025) are represented by corresponding different vibrational modes.

V. RESULTS

The Raman spectra were collected from the hematite crystal and jasper as silicate matrix using solid state Nd:YAG laser (532 nm) attached with Raman-SNOM-AFM Microscope System operating between 0.3 to 1 mW output power. The acquisition region of spectra extended from Raman Shift 100 to 3500 cm^{-1}, which have been normalized.

The reddish brown colour silicate matrix (SiO_2) or Jasper is characterized by four diagnostic Raman peaks at approximately 128, 208, 466 and 1318 cm^{-1} with feeble intensities (Fig. 4b). The Raman Shift near 128 cm^{-1} in Jasper is attributed to an E mode represent doubly degenerate vibrational mode (phonons) whereas Raman Shift near 208 cm^{-1} produce Raman active A1 vibrational mode (Li et al., 2025). The characteristic Raman Shift 466 cm^{-1} in Jasper is arise due symmetric stretching vibration of four membered rings of SiO_4-tetrahedra crystal structure (Gillet et al., 1990).

The hematite crystal is characterized by five diagnostic Raman peaks at approximately 222, 288, 406, 604 and 1318 cm^{-1} with very strong intensities in the range of 100 to 1500 cm^{-1} (Fig. 4c). The Raman Shift about 222 cm^{-1} position is attributed to A1g vibrational mode of Fe_2O_3 phase (De Faria et al., 1997). The Raman Shift at nearly 288, 406 and 604 cm^{-1} are attributed to Eg vibrational mode of Fe_2O_3 phase (Cao et al., 2006). Changes in the intensities of Raman Shift observed in the natural samples can be explained by presence of crystalline nature more sensitive Raman scattering effect.

There is a common Raman Shift position observed at approximately 1318 cm^{-1} in the jasper and hematite with variable intensities because of similar molecular vibrational modes with relatively different level of responses. The Raman Shift at approximately 1318 cm^{-1} is strongly arise by two-phonon longitudinal optical (2LO) scattering process induced by vibrational modes of Fe-O in the crystallographic structure (Marshall & Dufresne, 2022). Variable intensities of Raman Shift at approximately 1318 cm^{-1} are observed in this study possible due to relatively different proportion of Fe-O component present in the jasper and hematite.

The Raman Shift 466 cm^{-1} and Raman Shift 1318 cm^{-1} are used to characterized vibrational modes of jasper as silicate matrix (Liu et al., 1997) and hematite crystal (Marshall et al., 2025), respectively (Fig. 5a). However, characteristic Raman Shift overlaps for different vibrational modes and extraction of band intensity, linewidth and peak positions becomes problematic to distinguish. This leading to significant ambiguity in the Raman scanning, mapping and imagining of natural mineral grains. According the Liu et al (1997), the Raman Shift 466 cm^{-1} is the most intense peak has been assigned to the vibrational stretching mode (Si-O-Si) of the four membered rings of SiO_4-tetrahedra in the jasper matrix. The characteristic Raman Shift 466 cm^{-1} is used for Raman mapping to show distribution of jasper matrix in the BHJ sample (Fig. 5b). According to Marshall et al (2025), the Raman Shift 1318 cm^{-1} is assigned to longitudinal optical phonon Raman scattering (Fe-O) in the crystal structure of hematite (Fe_2O_3). The characteristic Raman Shift 1318 cm^{-1} is applied for Raman mapping to displays hematite crystal in the sample of BHJ (Fig. 5c).

In this study, characteristic Raman Shift selected for jasper and hematite is applied to understand the crystal structure in the BHJ. Euhedral hematite crystal is perfectly grown inside the jasper matrix possible due to the nucleation of Fe_2O_3 phase and uniform crystal growth rate of hematite in the jasperous matrix for

restricted time period. Growth of large size crystal requires long time with uniform crystal growth rate. Crystal size is directly proportional to the time of uniform crystal growth rate in a homogenous supersaturated solution. The size of the hematite crystal strongly depends on the concentration of Fe_2O_3 phase in the jasperous matrix.

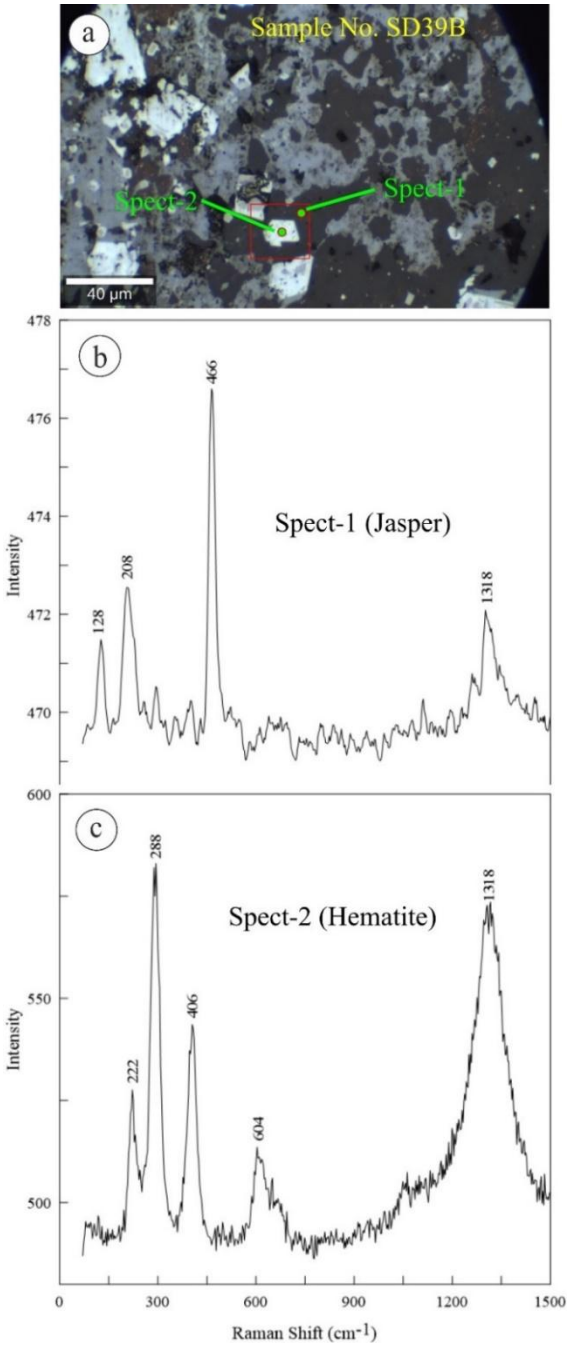

Fig. 4. (a) Representative photomicrograph shows hematite crystal in the matrix of jasper. (b) Characteristic Raman spectra of jasper and (c) hematite crystal in the BIF sample from Agori Formation.

The LRMS measurements intrinsically contain uncertainties and probable errors. These can ascend from numerous sources, including instrument limitations, sample physical characteristics, and data analysis methods. Understanding these factors and enumerating their impact is critical for precise interpretation of Raman spectra. Ambiguity is connected to peak intensity, noise, and spectral resolution, which comparatively impacts error in the LRMS measurements (Saltonstall et al., 2019). In this study, Raman mapping can accomplish with an accuracy ±5 cm^{-1}, which is appropriate for recognizing and depicting different chemical phases and their vibrational modes.

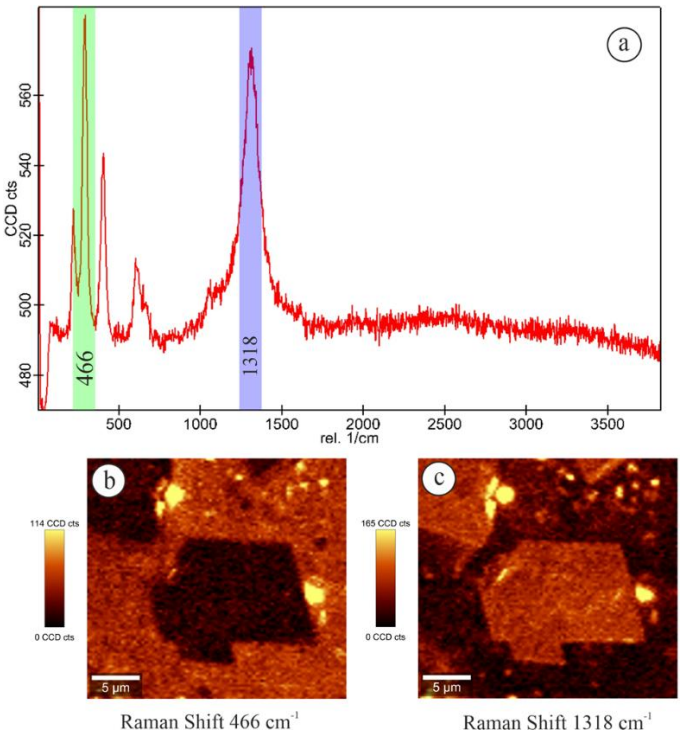

Fig. 5. (a) Representative Raman spectrum using SNOM for the hematite crystal on the sample of BIF from Agori Formation. (b) Scanning with mapping over Raman Shift 466 cm^{-1} and (c) mapping over Raman Shift 1318 cm^{-1} for the euhedral hematite crystal in the BIF sample from Agori Formation.

VI. DISCUSSIONS

In the MGB in Central India is known for hosting various mineralization's including iron ore associated with BHJ and BHQ. The occurrence of BHJ indicates probable iron ore deposits. In this study, hematite is identified as the major iron oxide mineral associated with jasperous matrix, which is found within Agori Formation. Euhedral to subhedral hematite crystals of various size ranges from nanoscale to microscale (i.e., <1 to 50 µm scale), which appears in the form of alternative bands with respect to jasper. The BHJ are result of chemical depositions by dichotomous sedimentation of irregular, silica-rich and iron-rich bands with variable thicknesses (Klein, 2005). However, these bands were developed as macrobands, mesobands and microbands in three various scales of layers known in BHJ (Li,

2014). This indicates geological processes with varying sedimentary rhythmites with thinnest microbands are 50 µm thick (Morris, 1993). The white colour bands and scattered hematite crystals shown in Fig. 4a. Single hematite crystals ranging from 10 to 50 µm in size. Microbands displayed of clusters of single hematite crystals were observed in the jasperous matrix of BHJ samples from Agori Formation. Euhedral hematite crystals are formed within the jasperous matrix through crystal nucleation and crystal growth. Hematite crystal growth can occur through various pathways, often involving the formation of intermediate phases (Scheck et al., 2019). Hematite is a mineral composed of iron oxide (Fe_2O_3), often forms through the oxidation of iron-containing phases in water. Hematite crystals can form within jasper-rich matrix through various geological processes. These processes include the precipitation of iron oxides as hematite crystals from iron-rich solutions, which can occur in chemical rich sedimentary environments or during hydrothermal processes.

CONCLUSIONS

The microbands of hematite crystals with thickness between 50 to 100 µm were observed in the BHJ sample from the Agori Formation of MGB. These microbands were found in the jasperous matrix or cryptocrystalline silica in the form of chert. Petrographic results indicates that the microbands of hematite crystals in jasper represent the Fe-rich and Si-rich layers precursors sequentially chemical precipitate, possibly driven by varying atmospheric O_2 conditions (Zhou et al., 2024). The LRMS study suggest that the euhedral hematite crystal in the jasperous matrix can grow through the precipitation of iron oxides from iron-rich solutions, hydrothermal processes, or other physico-chemical processes in marine environment. The specific crystal nucleation and crystal growth processes and resulting crystal forms can vary depending on the local physicochemical conditions of the Precambrian Ocean and atmosphere (Rasmussen et al., 2014). The textural evidence is very useful to understand the feasibility of crystallization such as microstructures, polymorphism and supersaturated solutions, which necessitates the inhibition of crystal nucleation and crystal growth (Zhang et al, 2024). Crystal nucleation and crystal growth during precipitation of hematite in the BHJ of Agori Formation precursors sequentially required supersaturated Fe-rich and Si-rich solution, uniform temperature and pressure conditions in the Paleoproterozoic Ocean and atmosphere.

ACKNOWLEDGMENT

The authors acknowledged to the Head of the Department, Department of Geology, Institute of Science, Banaras Hindu University (BHU) for providing necessary facilities. AKS acknowledged UGC sponsored Junior Research Fellowship. DP acknowledged financial support from BHU-IoE sponsored SEED Grant and BHU-IoE sponsored Professional Development Fund (PDF).

REFERENCES

Cao, H., Wang, G., Zhang, L., Liang, Y., Zhang, S. & Zhang, X. (2006) Shape and magnetic properties of single-crystalline hematite (α-Fe_2O_3) nanocrystals. ChemPhysChem, 7, 1897-1901. DOI: 10.1002/cphc.200600130.

De Faria, D.L.A., Silva, S.V. & De Oliveira, M.T. (1997) Raman Microspectroscopy of some iron oxides and oxyhydroxides. Journal of Raman Spectroscopy, 28, 873-878.

Egglseder, M.S., Cruden, A.R., Tomkins, A.G., Wilson, S.A., Dalstra, H.J., Rielli, A., Li, C., Baumgartner, J. & Faivre, D. (2019) Tiny particles building huge ore deposits-particle-based crystallisation in banded iron formation-hosted iron ore deposits (Hamersley Province, Australia). Ore Geology Review, 104, 160-174. https://doi.org/10.1016/j.oregeorev.2018.10.001.

Ferraro, J.R., Nakamoto, K. & Brown, C.W. (2003). Introductory Raman Spectroscopy. Academic Press, San Diego, CA., pp 1-434.

Gillet, Cleach, A.L. & Madon, M. (1990) High-temperature Raman Spectroscopy of SiO_2 and GeO_2 polymorphs: anharmonicity and thermodynamic properties at high-temperature. Journal of Geophysical Research, 95, 21635-21655.

Klein, C. (2005) Some Precambrian banded iron-formations (BIFs) from around the world: Their age, geologic setting, mineralogy, metamorphism, geochemistry, and origins. American Mineralogist, 90 (10). pp. 1473-1499. DOI 10.2138/am.2005.1871.

Lafuente, B., Downs, R.T., Yang, H., & Stone, N. (2015). The power of databases: the RRUFF project. In: Highlights in Mineralogical Crystallography, T Armbruster & R M Danisi, eds. Berlin, pp 1-30.

Li, J., Chou, I.M., Wang, X., Liu, Y., Han, Z. & Gao, J. (2025) Pressure sensor based on the Raman shift of the 128-cm^{-1} band of quartz for pressure measurements in hydrothermal diamond-anvil cells. Chemical Geology, 674, 122558. https://doi.org/10.1016/j.chemgeo.2024.122558.

Li, Y.L. (2014) Micro- and nanobands in late Archean and Palaeoproterozoic banded-iron formations as possible mineral records of annual and diurnal depositions. Earth and Planetary Science Letters, 391, 160–170. http://dx.doi.org/10.1016/j.epsl.2014.01.044.

Liu, L., Mernagh, T.P. & Hibberson, W.O. (1997) Raman spectra of high-pressure polymorphs of SiO2 at various temperatures. Physics and Chemistry of Minerals, 24, 396-402.

Marshall, C.P. & Dufresne, W.J.B. (2022) Resonance Raman and polarized Raman scattering of single-crystal hematite. Journal of Raman Spectroscopy, 53, 947-955. DOI: 10.1002/jrs.6309.

Marshall, C.P., Stockdale, G. & Carr, C.A. (2025) Raman Spectroscopy of geological varieties of hematite of varying

crystallinity and morphology. Journal of Raman Spectroscopy, 56, 590-597. https://doi.org/10.1002/jrs.6811.

Mernagh, T.P. & Trudu, A.G. (1993). A laser Raman microprobe study of some geologically important sulphide minerals. Chemical Geology, 103, 113-127.

Misra, P.S., Pandit, D., Murmu, A.K, Saleesh, P.N. & Salu, S., (2022). Bismuth–Telluride-Gold mineralisation from Parsoi area in Eastern Mahakoshal belt, Sonbhadra District, UP, India. Journal Geological Society of India, 98, 198-202.

Morris, R.C. (1993) Genetic modeling for banded iron-formation of the Hamersley Group, Pilbara Carton, Western Australia. Precambrian Research, 60, 243-286.

Pasteris, J.D., Freeman, J.J., Goffredi, S.K. & Buck, K.R. (2001). Raman spectroscopic and laser scanning confocal microscopic analysis of sulfur in living sulfur-precipitating marine bacteria. Chemical Geology, 180, 3–18.

Rasmussen, B., Krapez, B. & Meier, D.B. (2014) Replacement origin for hematite in 2.5 Ga banded iron formation: Evidence for postdepositional oxidation of iron-bearing minerals. Geological Society of America Bulletin, 126, 438-446. doi: 10.1130/B30944.1.

Roy, A., Prasad, M.H. & Devarajan, M.K. (2002a). Low pressure metamorphism, deformation and syntectonic granite emplacement in the Palaeoproterozoic Mahakoshal supracrustal belt, Central India. Gondwana Research, 5, 489-500.

Saltonstall, C.B., Beechem, T.E., Amatya, J., Floro, J., Norris, P.M. & Hopkins, P.E. (2019). Uncertainty in linewidth quantification of overlapping Raman bands. Review of Scientific Instruments, 90, 013111. doi: 10.1063/1.5064804.

Scheck, J., Fuhrer, L.M., Wu, B., Drechsler, M. & Gebauer, D. (2019) Nucleation of Hematite: A Nonclassical Mechanism. Chemistry A European Journal, 25(56), 13002-13007. https://doi.org/10.1002/chem.201902528.

Shanker, S. (1991) Thermal and crustal structure of "SONATA". A zone of mid continental rifting in Indian Shield. Journal Geological Society of India, 37, 211-220.

Zhang, Y., Li, B., Liu, J., Han, D., Rohani, S., Gao, Z. & Gong, J. (2024) Inhibition of Crystal Nucleation and Growth: A Review. Crystal Growth & Design, 24, 2645-2665. https://doi.org/10.1021/acs.cgd.3c01345.

Zhou, T., Hill, T.R., Roden, E.E. & Xu, H. (2024) The felsic volcanism associated BIF-like iron formations: Their origin and implication for BIFs. Chemical Geology, 656, 122091. https://doi.org/10.1016/j.chemgeo.2024.122091.

*****